

# An Improved Parameterized Approach for Real Time Optimal Motion Planning of AUV Moving in Dynamic Environment

Wenhao Luo<sup>1</sup>, Jun Peng<sup>2,\*</sup> and Jing Wang<sup>3</sup>

**Abstract**—In this paper, we present an improved analytic method to the optimal trajectory generation of an autonomous underwater vehicle (AUV) in a dynamic environment. The proposed approach explicitly incorporates both the AUV kinematic and the geometric constraints due to dynamic obstacles and the terrain while rendering the near-shortest path by a performance index related to the path length. In particular, the proposed design is based on a family of parameterized trajectories determined by three adjustable parameters, which provides a unified way to reformulate the geometric constraints and performance index into a set of parameterized constraint equations. To that end, such a constrained optimization problem boils down to optimize those adjustable parameters, which can be analytically solved in the parameter space. The proposed solution enhances the methodologies of real-time path planning for robots in 3D environment. Simulation results verify the effectiveness of the proposed method.

## I. INTRODUCTION

For the motion planning problem, there are several issues to be considered in order to generate a desirable path, including robot kinematic constraints, collision avoidance criterion, optimization on energy or path length, etc as introduced in [1]. To design a desired motion planner for the AUV in 3D cluttered dynamic space, we may hope to simultaneously take feasibility and optimality problems into account and ensure the computational efficiency for on-line planning.

Many efforts have been imposed towards motion planning in 3-D space with methods extended from 2D planning. For example, the method of potential field first proposed in [2] has been widely used. The basic idea is to construct virtual potential fields around obstacles and pathways to push the trajectory from obstacles and navigate the vehicle towards the terminal position. In order to address motion planning problem in 3-D environment and deal with the canonical local minima drawback, follow-up work can be found in [3]. However, when applied in 3-D environment, the amount of computation could increase largely. Also, the existence of potential minima may weaken the potential field method towards on-line motion planning in the 3-D space.

<sup>1</sup>W. Luo is with the Department of Automation, Shanghai Jiao Tong University, and Key Laboratory of System Control And Information Processing, Ministry of Education of China, Shanghai, 200240, China (e-mail: whluo@sjtu.edu.cn).

<sup>2</sup>J. Peng is with the School of Information Science and Engineering, Central South University, and Hunan Engineering Laboratory for Advanced Control and Intelligent Automation, Changsha, 410083, China (e-mail: pengj@csu.edu.cn).

\*Corresponding Author: J. Peng, pengj@csu.edu.cn

<sup>3</sup>J. Wang is with the Computer Engineering Program, Bethune-Cookman University, Daytona Beach, FL 32114 USA (e-mail: wangj@cookman.edu).

Other works have focused on techniques in computational geometry using a grid such as [4]. A shortcoming of many grid-based approaches is that the generated path is often restricted to track multiples of 45 degree angles only. To that end, the resultant path can be suboptimal and may contain false turns. To fast find out possible paths, the rapidly random tree exploring(RRT) method [5] is introduced to search feasible and optimal paths, and address both vehicle's kinematic and kinodynamic constraints. But in 3-D dynamic environment, it may take time to converge to optimal paths due to the random process.

For the purpose of efficient computation, [6] proposes an approximate numerical method to deal with real-time planning. A more desirable analytic method to solve real-time planning is pioneered in [7]. Later in [8] energy-optimal and path length-optimal problems are addressed in closed form. [9][10] modify canonical analytic solution for the purpose of motion planning in 3-D space. However, lack of consideration on higher dimensional states makes the reference control inputs discrete and nonsmooth. Nonetheless, the idea of parametric method is ideal to fast compute feasible paths for real-time planning.

In this paper, the basic idea of parametric trajectory generation is followed. An improved analytical solution is proposed to solve optimization motion planning for AUV in dynamic environment. By parameterizing the family of trajectories as three polynomials, the kinematic constraints of AUV can be handled together with geometric constraints. The trajectory generation problem can then be recast as determining three freely adjustable parameters based on a set of constraint equations. The optimization problem redefined in the parameter space unifies the discussion of collision-avoidance criterion and performance index. The suboptimal solution can be periodically updated to incorporate dynamic environment. Simulation results verify the validity and superiority of the proposed method.

This paper is organized as follows. Section II introduces the AUV model, environment model and the optimal motion planning problem. In section III, optimal solution and collision avoidance amidst obstacles will be analytically considered and combined to compute desired optimal path through the parameter space. Simulation results are shown and discussed in section IV to prove the effectiveness of the approach. In section V, conclusions are drawn.

## II. PROBLEM FORMULATION

The AUV model is shown in Fig.1. It can be represented by its circumsphere and conforms to the kinematic

constraints. The position and posture of the AUV can be described by the coordinate  $(x, y, z)$  of the circumsphere center CP and the  $Z-Y-X$  Euler angles  $(\psi, \theta, \phi)$  (Yaw-Pitch-Roll).

Then one can obtain the following kinematic model for

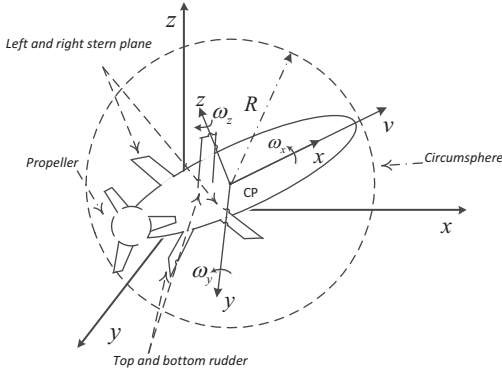


Fig. 1. Autonomous Underwater Vehicle Model

the AUV:

$$\begin{bmatrix} \dot{x} \\ \dot{y} \\ \dot{z} \end{bmatrix} = \begin{bmatrix} \cos\theta \cos\psi \\ \cos\theta \sin\psi \\ \sin\theta \end{bmatrix} u_v^T \quad (1)$$

$$\begin{bmatrix} \dot{\phi} \\ \dot{\theta} \\ \dot{\psi} \end{bmatrix} = \begin{bmatrix} 1 & \sin\phi \tan\theta & \cos\phi \tan\theta \\ 0 & \cos\phi & -\sin\phi \\ 0 & \sin\phi \sec\theta & \cos\phi \sec\theta \end{bmatrix} u_\omega^T \quad (2)$$

where the input is  $u = (u_v, u_\omega)^T$ , which includes linear velocity vector  $u_v$  and rotation velocity vector  $u_\omega$ .  $u_v = v$  is the thrust velocity along the vehicle fuselage.  $u_\omega = (\omega_x, \omega_y, \omega_z)$  contains corresponding rotation angular velocities of the AUV around three coordinate axis in 3-D Cartesian Space.

For motion planning problem, an expected planner should drive the AUV along an optimal trajectory from initial condition  $q^0 = (x_0, y_0, z_0, \phi_0, \theta_0, \psi_0)^T$  at time  $t_0$  to terminal condition  $q^f = (x_f, y_f, z_f, \phi_f, \theta_f, \psi_f)^T$  at time  $t_f$  in a dynamical changing environment within the given maneuver time  $T = t_f - t_0$ . Consider the kinematic constraints of AUV and geometric constraints due to the dynamic or static obstacles, the problem can be formulated as follows:

$$\begin{aligned} & \min J(q, \dot{q}) \\ & \text{s.t. } q(t_0) = q^0 \\ & \quad q(t_f) = q^f \\ & \quad M(q, \dot{q}) = 0 \\ & \quad F(x(t), y(t), z(t)) \geq 0 \end{aligned} \quad (3)$$

where  $J(q, \dot{q})$  is a performance index to achieve optimal control such that the generated trajectory is the shortest.  $M(q, \dot{q})$  represents the kinematic constraints of AUV.  $F(x(t), y(t), z(t))$  indicates geometric constraints obtained

from collision avoidance of both terrain and dynamic obstacles.

For convenience, we assume the terrain environment is represented by flat terrain with ellipsoid-like obstacles. The dynamic obstacles are shown by spheres moving with linear velocity at each sampling interval. Motions and positions of the obstacles can be detected within sensors on the AUV. The environment is then formulated in Fig.2.

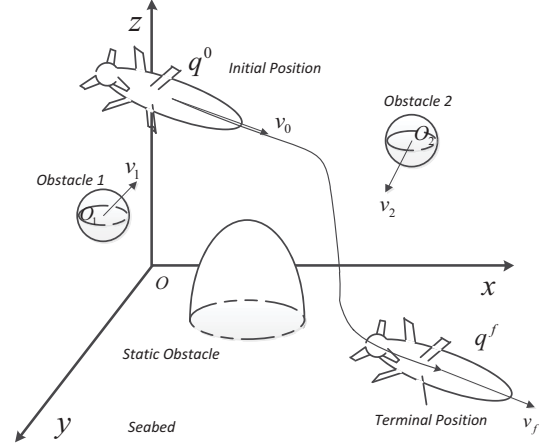


Fig. 2. AUV moving in a dynamic environment.

### III. REAL-TIME OPTIMAL TRAJECTORY GENERATION FOR AUV

#### A. Feasible Trajectory Generation for an AUV without Constraints

To address the motion planning problem, first we discuss the parameterized trajectory model of AUV. Idea of parametric trajectory method in [7][9] is followed, and we specify the trajectories by three independent piece-wise parameterized polynomials with respect to time  $t$ , rather than geometric variables in [9]. Then the family of trajectories can be given as follows.

$$\begin{aligned} x(t) &= [c_0 \ c_1 \ c_2 \ \dots \ c_p] f(t) \\ y(t) &= [d_0 \ d_1 \ d_2 \ \dots \ d_p] f(t) \\ z(t) &= [e_0 \ e_1 \ e_2 \ \dots \ e_p] f(t) \end{aligned} \quad (4)$$

where

$$f(t) = [1 \ t \ t^2 \ t^3 \ \dots \ t^p]^T \quad (5)$$

In (4),  $x(t)$ ,  $y(t)$  and  $z(t)$  are the coordinates of AUV's position and integer  $p > 0$  is an undetermined order. Typically,  $p = 3$  suffices to generate a unique path under given boundary conditions. To incorporate collision avoidance property and overcome discrete control drawbacks in [9][10], we raise the order  $p$  to be 6, which could also improve the optimal performance for the generated trajectory. Recalling the kinematic model in (1), the kinematic constraints on the translational motion of the AUV can be obtained as follows.

$$\theta = \arctan \frac{\dot{z}}{\sqrt{(\dot{x}^2 + \dot{y}^2)}}, \quad \psi = \arctan \frac{\dot{y}}{\dot{x}} \quad (6)$$

Moreover, so as to maintain the AUV to be upright, it is found that  $\phi = \phi_0 e^{-kt}$  as defined in [9]. Then, combining equation (1), (2) and (6), we have the formulas of the control inputs as follows.

$$\begin{aligned}
u_v &= \pm \sqrt{\dot{x}^2 + \dot{y}^2 + \dot{z}^2} \\
\omega_x &= \phi_0 e^{-kt} - \frac{(\ddot{y}\dot{x} - \dot{y}\ddot{x})\dot{z}}{(\dot{x}^2 + \dot{y}^2)\sqrt{\dot{x}^2 + \dot{y}^2 + \dot{z}^2}} \\
\omega_y &= \frac{\ddot{y}\dot{x} - \dot{y}\ddot{x}}{\sqrt{(\dot{x}^2 + \dot{y}^2)(\dot{x}^2 + \dot{y}^2 + \dot{z}^2)}} \sin(\phi_0 e^{-kt}) \\
&\quad + \frac{\ddot{z}(\dot{x}^2 + \dot{y}^2) - \dot{z}(\dot{x}\ddot{x} + \dot{y}\ddot{y})}{\sqrt{(\dot{x}^2 + \dot{y}^2)(\dot{x}^2 + \dot{y}^2 + \dot{z}^2)}} \cos(\phi_0 e^{-kt}) \\
\omega_z &= \frac{\ddot{y}\dot{x} - \dot{y}\ddot{x}}{\sqrt{(\dot{x}^2 + \dot{y}^2)(\dot{x}^2 + \dot{y}^2 + \dot{z}^2)}} \cos(\phi_0 e^{-kt}) \\
&\quad - \frac{\ddot{z}(\dot{x}^2 + \dot{y}^2) - \dot{z}(\dot{x}\ddot{x} + \dot{y}\ddot{y})}{\sqrt{(\dot{x}^2 + \dot{y}^2)(\dot{x}^2 + \dot{y}^2 + \dot{z}^2)}} \sin(\phi_0 e^{-kt})
\end{aligned} \tag{7}$$

If one specific trajectory has been solved in the form of (4), then the derivatives of the obtained trajectory expressions can be directly substituted to (6) and (7), which thereby renders the reference intermediate posture and the correspondent control inputs at each moment for the AUV to track such a path.

To make control inputs continuous, we assume the control inputs  $u = (u_v, u_\omega)^T$  at boundary time  $t_0$  and  $t_f$  are known. Then, from kinematic and input equations in (1) and (7), the original boundary conditions  $q^0$  and  $q^f$  can be reformulated as three redefined boundary conditions as follows.

$$\begin{aligned}
q_x &= \left( \begin{array}{cccc} x_0 & x_f & \frac{dx}{dt} \Big|_{t_0} & \frac{dx}{dt} \Big|_{t_f} \\ y_0 & y_f & \frac{dy}{dt} \Big|_{t_0} & \frac{dy}{dt} \Big|_{t_f} \\ z_0 & z_f & \frac{dz}{dt} \Big|_{t_0} & \frac{dz}{dt} \Big|_{t_f} \end{array} \right) \\
q_y &= \left( \begin{array}{cccc} \frac{d^2x}{dt^2} \Big|_{t_0} & \frac{d^2x}{dt^2} \Big|_{t_f} & \frac{d^2y}{dt^2} \Big|_{t_0} & \frac{d^2y}{dt^2} \Big|_{t_f} \\ \frac{d^2z}{dt^2} \Big|_{t_0} & \frac{d^2z}{dt^2} \Big|_{t_f} & & \end{array} \right) \\
q_z &= \left( \begin{array}{cccc} & & & \end{array} \right)
\end{aligned} \tag{8}$$

Therefore, by considering those redefined boundary conditions, coefficients in (4) can be solved by three independent parameters to generate a class of feasible trajectories without consideration of constraints, as discussed in the following Theorem 1. To further consider the dynamic environment, we assume the piecewise-constant parameterized trajectory (4) is determined within every sampling time interval  $t \in [t_0 + kT_s, t_0 + (k+1)T_s]$  ( $k = 0, 1, \dots, \bar{k} - 1$ ), coefficients  $c_i^k$ ,  $d_i^k$  and  $e_i^k$ ,  $i = 0, \dots, 6$  are constants, where  $T_s$  is the sampling time, and  $\bar{k}$  is the maximum integer less than  $T/T_s$ . Then the redefined boundary condition in (8) can be substituted to trajectory in (4), which renders new trajectory model as in following straightforward Theorem.

**Theorem 1:** For  $t \in [t_k, t_f]$ ,  $t_k = t_0 + kT_s$ , the parameterized trajectory for the vehicle can be described as

$$\begin{aligned}
x(t) &= \bar{f}(t)(G^k)^{-1}(E^k - H^k c_6^k) + c_6^k t^6 \\
y(t) &= \bar{f}(t)(G^k)^{-1}(F^k - H^k d_6^k) + d_6^k t^6 \\
z(t) &= \bar{f}(t)(G^k)^{-1}(I^k - H^k e_6^k) + e_6^k t^6
\end{aligned} \tag{9}$$

where  $\bar{f}(t) = [1 \ t \ t^2 \ t^3 \ t^4 \ t^5]$ , and

$$\begin{aligned}
G^k &= \begin{bmatrix} 1 & t_k & t_k^2 & t_k^3 & t_k^4 & t_k^5 \\ 1 & t_f & t_f^2 & t_f^3 & t_f^4 & t_f^5 \\ 0 & 1 & 2t_k & 3t_k^2 & 4t_k^3 & 5t_k^4 \\ 0 & 1 & 2t_f & 3t_f^2 & 4t_f^3 & 5t_f^4 \\ 0 & 0 & 2 & 6t_k & 12t_k^2 & 20t_k^3 \\ 0 & 0 & 2 & 6t_f & 12t_f^2 & 20t_f^3 \end{bmatrix} \\
E^k &= \left[ \begin{array}{cccccc} x_k & x_f & \frac{dx}{dt} \Big|_{t_k} & \frac{dx}{dt} \Big|_{t_f} & \frac{d^2x}{dt^2} \Big|_{t_k} & \frac{d^2x}{dt^2} \Big|_{t_f} \end{array} \right]^T \\
F^k &= \left[ \begin{array}{cccccc} y_k & y_f & \frac{dy}{dt} \Big|_{t_k} & \frac{dy}{dt} \Big|_{t_f} & \frac{d^2y}{dt^2} \Big|_{t_k} & \frac{d^2y}{dt^2} \Big|_{t_f} \end{array} \right]^T \\
I^k &= \left[ \begin{array}{cccccc} z_k & z_f & \frac{dz}{dt} \Big|_{t_k} & \frac{dz}{dt} \Big|_{t_f} & \frac{d^2z}{dt^2} \Big|_{t_k} & \frac{d^2z}{dt^2} \Big|_{t_f} \end{array} \right]^T \\
H^k &= \left[ \begin{array}{cccccc} t_k^6 & t_f^6 & 6t_k^5 & 6t_f^5 & 30t_k^4 & 30t_f^4 \end{array} \right]^T
\end{aligned} \tag{10}$$

It should be noted that since  $t_k$  will not be equal to  $t_f$ , matrix  $G^k$  in (10) could avoid singularity problems. Now, the first three constraints in (3) have been addressed. It follows from the parameterized trajectory in (9) that the motion planning boils down to solve for  $c_6^k$ ,  $d_6^k$  and  $e_6^k$  based on constraints due to collision avoidance and performance, which can be uniformly solved by analytical solutions formulated in a parameter space in next subsections.

### B. Optimal Solution to Feasible Paths without Obstacles

Recall equation (9) in Theorem 1, it is straightforward that arbitrary selection of  $c_6^k$ ,  $d_6^k$  and  $e_6^k$  can render a class of kinematically feasible trajectories for AUV. To evaluate the arc length of the generated trajectory, we can employ the integral of thrusting velocity  $|u_v|$  of AUV with respect to time as the performance index of path:

$$J_k^0(c_6^k, d_6^k, e_6^k) = \int_{t_k}^{t_f} |u_v| dt = \int_{t_k}^{t_f} \sqrt{\dot{x}^2 + \dot{y}^2 + \dot{z}^2} dt \tag{11}$$

However, no analytic solution of  $(c_6^k, d_6^k, e_6^k)$  can be obtained from (11). In order to maintain validity of the performance index while making it easier to compute the solution, we use the quadratic form of (11) to represent the path length. Then the modified index is as follows.

$$J_k(c_6^k, d_6^k, e_6^k) = \int_{t_k}^{t_f} u_v^2 dt = \int_{t_k}^{t_f} (\dot{x}^2 + \dot{y}^2 + \dot{z}^2) dt \tag{12}$$

To this end, the optimization problem becomes

$$\min J_k(c_6^k, d_6^k, e_6^k) \tag{13}$$

And the analytic optimal solution can be obtained by the following Theorem.

**Theorem 2:** At each time instant  $t_k = t_0 + kT_s$ , the optimization problem (13) is always solvable, and its solutions are

$$c_6^{k*} = -s_1^k / (2s_2^k), \quad d_6^{k*} = -s_4^k / (2s_2^k), \quad e_6^{k*} = -s_5^k / (2s_2^k) \tag{14}$$

where  $s_1, s_2, s_4$  and  $s_6$  are given in equations (16).

*Proof:* Since  $\dot{x}, \dot{y}$  and  $\dot{z}$  are also polynomials in terms of  $t$  and coefficients  $c_6^k, d_6^k$  and  $e_6^k$ , then the performance index can be rewritten as

$$\begin{aligned} J_k(c_6^k, d_6^k, e_6^k) &= \int_{t_k}^{t_f} (\dot{x}^2 + \dot{y}^2 + \dot{z}^2) dt \\ &= s_2^k \left( c_6^k + \frac{s_1^k}{2s_2^k} \right)^2 + s_2^k \left( d_6^k + \frac{s_4^k}{2s_2^k} \right)^2 + s_2^k \left( e_6^k + \frac{s_5^k}{2s_2^k} \right)^2 \\ &\quad + \left( s_0^k + s_3^k + s_6^k \right) - \frac{(s_1^k)^2 + (s_4^k)^2 + (s_5^k)^2}{4s_2^k} \end{aligned} \quad (15)$$

where

$$\begin{aligned} s_0^k &= \int_{t_k}^{t_f} (\bar{f}'(G^k)^{-1} E^k)^2 dt, \quad s_6^k = \int_{t_k}^{t_f} (\bar{f}'(G^k)^{-1} I^k)^2 dt \\ s_1^k &= 2 \int_{t_k}^{t_f} \left( 6t^5 - \bar{f}'(G^k)^{-1} H^k \right) (\bar{f}'(G^k)^{-1} E^k) dt \\ s_2^k &= \int_{t_k}^{t_f} \left( 6t^5 - \bar{f}'(G^k)^{-1} H^k \right)^2 dt, \quad s_3^k = \int_{t_k}^{t_f} (\bar{f}'(G^k)^{-1} F^k)^2 dt \\ s_4^k &= 2 \int_{t_k}^{t_f} \left( 6t^5 - \bar{f}'(G^k)^{-1} H^k \right) (\bar{f}'(G^k)^{-1} F^k) dt \\ s_5^k &= 2 \int_{t_k}^{t_f} \left( 6t^5 - \bar{f}'(G^k)^{-1} H^k \right) (\bar{f}'(G^k)^{-1} I^k) dt \\ \bar{f}' &= [0 \quad 1 \quad 2t \quad 3t^2 \quad 4t^3 \quad 5t^4] \end{aligned} \quad (16)$$

Since the integration terms of  $s_0^k \sim s_6^k$  are constant at each sampling instant, it follows from the last equation in (15) that  $J_k$  is minimized if the solution in (14) are applied. This completes the proof.  $\square$

Particularly, since the optimal solution is obtained in closed form and only related to boundary conditions, the optimal trajectory can be directly generated and updated at each sampling instant, which is good for real-time planning. Moreover, if we consider the optimal solutions (14) in a 3D parameter space of  $c_6 - d_6 - e_6$ , they become fixed points  $O^{k*}$  with coordinates  $(c_6^{k*}, d_6^{k*}, e_6^{k*})$ . According to the last equation in (15), for any candidate parameter sets  $O^k(c_6^k, d_6^k, e_6^k)$ , their corresponding trajectory performance can be evaluated immediately by the distance between  $O^{k*}$  and  $O^k$ . Such a property is employed in the discussion of suboptimal path with obstacles in the next subsection.

### C. Optimal Motion Planning for an AUV with Collision Avoidance Constraints

To better formulate the possible environment for the AUVs, two kinds of obstacles are incorporated as illustrated in Fig.2, i.e. the ellipsoid-like terrain and the dynamic obstacles covered by their circumspheres (including other AUVs). The AUV's velocity and radius are represented by  $v$  and  $R$ . During one sampling period  $t \in [t_0 + kT_s, t_0 + (k+1)T_s]$  (often small enough), velocity  $v_i^k$  of the  $i$ th dynamic obstacle (with radius  $r_i$ ) can be regarded as constant. The ellipsoid-like terrain is fixed in the flat. Motion changing of obstacles can be detected and updated at every sampling instant  $t = t_0 + kT_s$

such that piecewise polynomial parameterizations can be adapted to formulate the entire trajectory for AUV.

During  $t \in [t_0 + kT_s, t_f]$  if the  $i$ th dynamic obstacles is considered to be static at its original position  $(x_i^k, y_i^k, z_i^k)$  at  $t_k$ , and relative velocity of the AUV to the  $i$ th obstacle is defined as  $(v_{i,x}^k, v_{i,y}^k, v_{i,z}^k)$ , then the distance between center of the AUV and the  $i$ th obstacle must satisfy:

$$\left( x'_i(t) - x_i^k \right)^2 + \left( y'_i(t) - y_i^k \right)^2 + \left( z'_i(t) - z_i^k \right)^2 \geq (r_i + R)^2 \quad (17)$$

where  $x'_i(t) = x(t) - v_{i,x}^k \tau$ ,  $y'_i(t) = y(t) - v_{i,y}^k \tau$ ,  $z'_i(t) = z(t) - v_{i,z}^k \tau$  (relative position of the AUV with respect to the  $i$ th dynamic obstacle),  $\tau = t - (t_0 + kT_s)$ , for  $t \in [t_0 + kT_s, t_f]$ .

For the  $j$ th ellipsoid-like terrain obstacle, the collision avoidance criterion can be formulated as follows.

$$z(t) - z_j^h \geq -[(x(t) - x_j^h)^2 / m_j^2 + (y(t) - y_j^h)^2 / n_j^2] \quad (18)$$

where  $(x_j^h, y_j^h, z_j^h)$  is the coordinate of the peak position of the  $j$ th terrain obstacle.  $m_j$  and  $n_j$  are parameters that can be adjusted to incorporate different shapes of the obstacles.

Now, we can substitute trajectory model (9) of AUV to collision avoidance criterion in (17) and (18) in order to reformulate such constraints by constrained inequations in terms of  $c_6^k, d_6^k, e_6^k$  as follows.

For  $i$ th dynamic obstacle, the constrained set is denoted by  $\Omega_{d,i,t}^k$ :

$$\left( c_6^k + \frac{g_{1,i}^k(t)}{g_2^k(t)} \right)^2 + \left( d_6^k + \frac{g_{3,i}^k(t)}{g_2^k(t)} \right)^2 + \left( e_6^k + \frac{g_{4,i}^k(t)}{g_2^k(t)} \right)^2 \geq \frac{(r_i + r_0)^2}{(g_2^k(t))^2} \quad (19)$$

where

$$\begin{aligned} g_{1,i}^k(t) &= \bar{f}(G^k)^{-1} E^k - v_{i,x}^k \tau - x_i^k, \quad g_{2}^k(t) = t^6 - \bar{f}(G^k)^{-1} H^k \\ g_{3,i}^k(t) &= \bar{f}(G^k)^{-1} F^k - v_{i,y}^k \tau - y_i^k \\ g_{4,i}^k(t) &= \bar{f}(G^k)^{-1} I^k - v_{i,z}^k \tau - z_i^k, \quad \bar{f} = [1 \quad t \quad t^2 \quad t^3 \quad t^4 \quad t^5] \end{aligned} \quad (20)$$

For  $j$ th static terrain obstacle, the constrained set is denoted by  $\Omega_{s,j,t}^k$ :

$$e_6^k \geq l_{1,j}(t)(c_6^k)^2 + l_{2,j}(t)c_6^k + l_{3,j}(t)(d_6^k)^2 + l_{4,j}d_6^k + l_{5,j}(t) \quad (21)$$

where

$$\begin{aligned} l_{1,j}(t) &= -\frac{t^6 - \bar{f}(G^k)^{-1} H^k}{m_j^2}, \quad l_{2,j}(t) = -\frac{2(\bar{f}(G^k)^{-1} E^k - x_j^h)}{m_j^2} \\ l_{3,j}(t) &= -\frac{t^6 - \bar{f}(G^k)^{-1} H^k}{n_j^2}, \quad l_{4,j}(t) = -\frac{2(\bar{f}(G^k)^{-1} F^k - y_j^h)}{n_j^2} \\ l_{5,j}(t) &= -\frac{(\bar{f}(G^k)^{-1} E^k - x_j^h)^2}{m_j^2(t^6 - \bar{f}(G^k)^{-1} H^k)} - \frac{\bar{f}(G^k)^{-1} I^k - z_j^h}{t^6 - \bar{f}(G^k)^{-1} H^k} \\ &\quad - \frac{(\bar{f}(G^k)^{-1} F^k - y_j^h)^2}{n_j^2(t^6 - \bar{f}(G^k)^{-1} H^k)} \end{aligned} \quad (22)$$

The ranges of  $c_6^k, d_6^k$  and  $e_6^k$  are obtained from (19) and (21). Thus a class of feasible paths can be achieved under the

two sets of inequations. It is noticed that in  $c_6 - d_6 - e_6$  parameter space,  $\Omega_{d,i,t}^k$  can be plotted as the exterior region of a sets of spheres, and  $\Omega_{s,j,t}^k$  can be plotted as the exterior region of a sets of elliptic paraboloid at each moment. Then considering all the detected obstacles for  $t \in [t_0 + kT_s, t_f]$ , we could obtain the general constrained area  $\Omega_d^k$  and  $\Omega_s^k$  as follows.

$$\begin{cases} \Omega_d^k = \bigcap_{i=1}^{i_k} \Omega_{d,i,t}^k, & t \in [t_0 + kT_s, t_f] \\ \Omega_s^k = \bigcap_{j=1}^{j_k} \Omega_{s,j,t}^k, & t \in [t_0 + kT_s, t_f] \end{cases} \quad (23)$$

where  $i_k$  and  $j_k$  are the total number of detected dynamic and terrain static obstacles at  $t = t_k$  respectively. To this end, recalling the original problem (3) and the proof process in Theorem 2, we can reformulate the optimization problem in the  $c_6 - d_6 - e_6$  parameter space. If adjustable parameters of the class of candidate trajectories are denoted by point  $O^k(c_6^k, d_6^k, e_6^k)$ . Then the reformulated problem is:

$$\min \text{dis}\{O^k, O^{k*}\}, \quad s.t. O^k \in \Omega_d^k \cap \Omega_s^k \quad (24)$$

Such an optimization problem can be well solved in  $c_6 - d_6 - e_6$  parameter space by specifying the position of  $O^k$  so that it stays as close to the optimal point  $O^{k*}$ , while located in the intersection regions of constraints sets  $\Omega_d^k$  and  $\Omega_s^k$ . Moreover, the intersection regions can be considered by their projections on the three 2-D planes respectively so that it is easier to compute the analytic solutions. For example, when considering two dynamic obstacles and two static terrain obstacles, one can obtain the constrained area projected on the  $c_6 - d_6$  plane similar as illustrated in Fig.3.

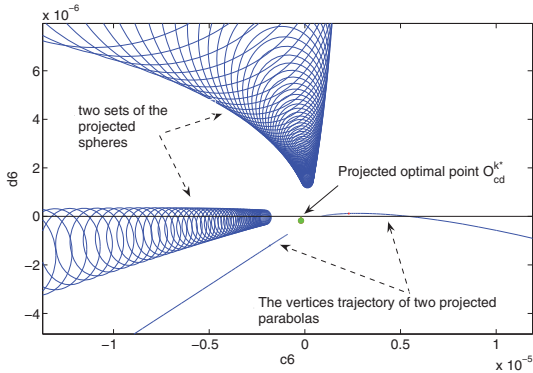


Fig. 3. Projections of optimal points, constraint spheres  $\Omega_d^k$  and the vertices trajectories of the constraint elliptic paraboloids  $\Omega_s^k$  on  $c_6 - d_6$  plane.

In Fig.3, the projected optimal point is located in the 'safety' area that is the exterior region of both the projected constraint sphere areas and elliptic paraboloid areas. In such particular case, the candidate solution  $(c_6^k, d_6^k, e_6^k)$  can be directly specified by  $(c_6^{k*}, d_6^{k*}, e_6^{k*})$ , and therefore renders the shortest path for AUV. Generally, once we obtain the constrained inequations (19) and (21), they can be projected on the three corresponding planes. Then based on optimal index in (24), one can choose the most desired suboptimal

solution according to the distance between the three candidate suboptimal points and the optimal point from respective planes. If only the feasible trajectory exists, one can always compute desired optimal or suboptimal paths based on the proposed approach.

#### IV. SIMULATION

This section describes the simulation results to verify the effectiveness of our approach. First, we consider the situation that AUV moves in an unstructured environment without obstacles. Our approach is compared against other typical geometric analytical solutions. In this section, the scales are the same. All quantities conform to a given unit system. The settings are as follows:

- AUV settings:  $R=1$ .
- Boundary Conditions:  $q^0 = (0, 0, 0, \frac{\pi}{6}, \frac{\pi}{4}, \frac{\pi}{6})$  and  $q^f = (30, 20, 10, 0, \frac{\pi}{5}, \frac{\pi}{10})$ .
- Maneuver time:  $t_0=0, t_f=40s$ .

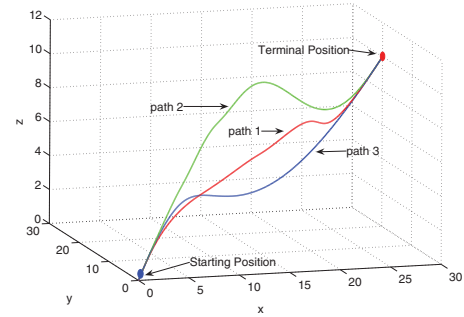


Fig. 4. The trajectories comparison of AUV without consideration of obstacles.

In Fig.4 there are three trajectories generated by our optimal approach (path 1) and typical analytic solutions under the minimum steering radius law (path 2) in [9] and the near-shortest path length principle (path 3) derived from [10]. It is straightforward that path 1 is the shortest one among the three paths. The minimum steering radius law can only be done numerically, which may render longer detours when the sampling interval is not short enough, as appeared on path 2. Path 3 performs better, but is still limited due to the lack of optimal flexibility on x-axis. In fact, after fitting different trajectory model, the parameter space can also be exploited to assess the optimality of analytic solutions in [9][10] as well.

To consider our optimal approach under dynamic environment, several static and dynamic obstacles are added to create a cluttered environment. Updated settings of such a scenario are as follows.

- Initial coordinates of the two moving obstacles:  $O_1(t_0) = [12.2, 5, 2.6]^T, O_2(t_0) = [22, 14, 9]^T$ .
- Initial settings for the two static terrain obstacle:  $O_{s1} = (5, 12, 5, 4, 9), O_{s2} = (17, 13, 10, 2, 2)$ .
- Radius of dynamic obstacles:  $r_i=1(i=1,2)$ .
- Boundary Conditions:  $q^0 = (0, 0, 0, \frac{\pi}{6}, \frac{\pi}{4}, \frac{\pi}{6})$  and  $q^f = (30, 20, 10, 0, \frac{\pi}{5}, \frac{\pi}{10})$ .  $u^0 = (1, 0.45, -0.04, 0.05)^T$  and  $u^f = (2, 0.01, 0.03, -0.01)^T$ .

- Starting time and ending time:  $t_0=0, t_f=40s$ .
- Velocities of the two moving obstacles from  $t=0s$  and change at  $t=10s$  and  $20s$  :  
 $v_1^0 = (-0.4, 0.4, 0.2)^T, v_1^1 = (0.2, -0.1, -0.4)^T, v_1^2 = (1, 0.2, 0.4)^T$   
 $v_2^0 = (0.1, 0.2, -0.1)^T, v_2^1 = (0.2, 0.2, -0.3)^T, v_2^2 = (-0.3, 0.4, -0.3)^T$   
 Sampling period is chosen to be  $T_s=10s$ .

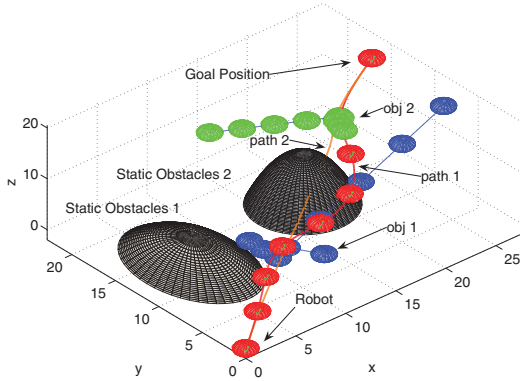


Fig. 5. The trajectories for the AUV in 3-D cluttered environment. .

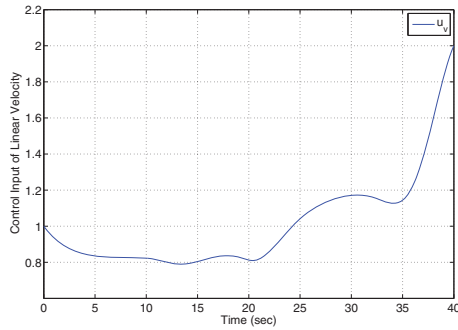


Fig. 6. The trajectory of the AUV thrusting velocity.

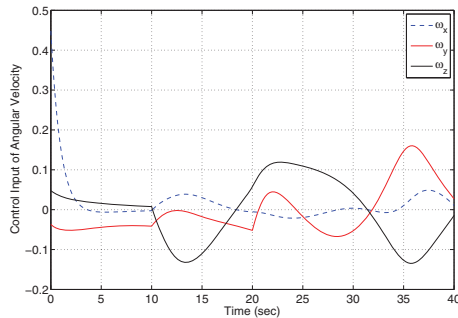


Fig. 7. The trajectory of three angular velocity inputs for the AUV.

In Fig.5, AUV is expected to move through the cluttered 3-D environment containing two moving obstacles and two static terrain ones with a near-shortest collision free path. The AUV and obstacles are marked by balls and half-ellipsoids in different colors. The moving spheres are drawn every 5 seconds. The red path 1 stands for the optimal trajectory

rendered by (24). The orange path 2 is identical to the optimal path 1 in Fig.4. The corresponding control inputs are plotted in Fig.6 and Fig.7. The original optimal path 2 collides with dynamic obstacle 1 and static obstacle 1 since it does not incorporate the obstacles. By updating the incoming information about obstacles' motion at each sampling instant, the red piece-wise path 1 can successfully avoid both static and dynamic obstacles, while fast converging to the original optimal path. In Fig.6 and Fig.7, the corresponding control inputs are stable and smooth, which makes it good for real-world applications.

## V. CONCLUSIONS

An improved analytical method is proposed to solve optimal trajectory generation problem for one AUV in dynamic 3-D cluttered environment. By reformulating the constrained optimization problem on a uniform 3-D parameter space, it is computationally efficient to calculate a near-shortest trajectory with consideration of kinematics constrain, boundary condition and collision avoidance criterion. The resultant control inputs are always continuous and the performance of the trajectories are better improved. The simulation results verify the effectiveness of our method.

## VI. ACKNOWLEDGMENT

The authors would like to acknowledge that this work is partially supported by National Natural Science Foundation of China No. 61071096, 61073103, 61003233, and Specialized Research Found for Doctoral Program of Higher Education No. 20100162110012 and No. 20110162110042.

## REFERENCES

- [1] S. M. LaValle, *Planning algorithms*. Cambridge University Press, 2006.
- [2] O. Khatib, "Real-time obstacle avoidance for manipulators and mobile robots," *The International Journal of Robotics Research*, vol. 5, no. 1, pp. 90–98, 1986.
- [3] J.-H. Chuang, "Potential-based modeling of three-dimensional workspace for obstacle avoidance," *IEEE Transactions on Robotics and Automation*, vol. 14, no. 5, pp. 778–785, 1998.
- [4] C. Petres, Y. Pailhas, P. Patron, Y. Petillot, J. Evans, and D. Lane, "Path planning for autonomous underwater vehicles," *IEEE Transactions on Robotics*, vol. 23, no. 2, pp. 331–341, 2007.
- [5] S. M. LaValle and J. J. Kuffner, "Randomized kinodynamic planning," *The International Journal of Robotics Research*, vol. 20, no. 5, pp. 378–400, 2001.
- [6] R. Prasanth Kumar, A. Dasgupta, and C. Kumar, "Real-time optimal motion planning for autonomous underwater vehicles," *Ocean Engineering*, vol. 32, no. 11, pp. 1431–1447, 2005.
- [7] Z. Qu, J. Wang, and C. E. Plaisted, "A new analytical solution to mobile robot trajectory generation in the presence of moving obstacles," *IEEE Transactions on Robotics*, vol. 20, no. 6, pp. 978–993, 2004.
- [8] J. Yang, Z. Qu, J. Wang, and K. Conrad, "Comparison of optimal solutions to real-time path planning for a mobile vehicle," *IEEE Transactions on Systems, Man and Cybernetics, Part A: Systems and Humans*, vol. 40, no. 4, pp. 721–731, 2010.
- [9] H. Yuan, J. Yang, Z. Qu, and J. Kaloust, "An optimal real-time motion planner for vehicles with a minimum turning radius," in *The Sixth World Congress on Intelligent Control and Automation*, vol. 1, 2006, pp. 397–402.
- [10] J. Yang, Z. Qu, J. Wang, and R. A. Hull, "Real-time optimized trajectory planning for a fixed-wing vehicle flying in a dynamic environment," *Journal of Aerospace Engineering*, vol. 22, no. 4, pp. 331–341, 2009.